chemistry proceedings

MDPI

Proceedings

Synthesis of New *bis*-furanyl-pyrrolo[3,4-*b*]pyridin-5-ones via the Ugi-Zhu Reaction and Docking Studies on the Main Protease (M^{Pro}) from SARS-CoV-2 †

Ivette Morales-Salazar [1], Sandra L. Castañón-Alonso [1], Daniel Canseco-González [2], Erik Díaz-Cervantes [3,*], Eduardo González-Zamora [1,*] and Alejandro Islas-Jácome [1,*]

[1] Departamento de Química, Universidad Autónoma Metropolitana-Iztapalapa, San Rafael Atlixco 186, Col. Vicentina, Iztapalapa, Ciudad de México C.P. 09340, Mexico; ivette649_tatu@hotmail.com (I.M.-S.); scastanon@xanum.uam.mx (S.L.C.-A.)

[2] Consejo Nacional de Ciencia y Tecnología—Laboratorio Nacional de Investigación y Servicio Agroalimentario y Forestal, Universidad Autónoma Chapingo, Km. 38.5 Carretera México-Texcoco, Chapingo C.P. 56230, México; jdcanseco@conacyt.mx

[3] Centro Interdisciplinario del Noreste (CINUG), Departamento de Alimentos, Universidad de Guanajuato, Tierra Blanca, Guanajuato C.P. 37975, Mexico

* correspondence: e.diaz@ugto.mx (E.D.-C.); egz@xanum.uam.mx (E.G.-Z.); aij@xanum.uam.mx (A.I.-J.)

† Presented at the 25th International Electronic Conference on Synthetic Organic Chemistry, 15–30 November 2021; Available online: https://ecsoc-25.sciforum.net (accessed on).

Abstract: The synthesis of five new *bis*-furanyl-pyrrolo[3,4-*b*]pyridin-5-ones in 30 to 40% yields through a domino sequence based on the Ugi-Zhu three-component reaction is described. Then, on the main protease M^{Pro} (PDB: 6lu7) from the SARS-CoV-2, the synthesized products and co-crystallized ligands of M^{Pro} were in silico evaluated using the docking technique, finding moderate to good binding energies and some interesting interactions, demonstrating that the ligand **8c** can be considered as a drug candidate against the SARS-CoV-2-M^{Pro} due to its LE value (−5.96 kcal/mol), which is better than other synthesized and reported molecules in the literature. At the same time, hydrophobic interactions play a crucial role in the ligand target molecular couplings, demonstrated through a hydrophobicity surfaces analysis. Finally, **8a** and **8b** can also be considered as drug candidates. Thus, some synthesized *bis*-furanyl-pyrrolo[3,4-*b*]pyridin-5-ones may be used for further in vitro assays against the virus.

Keywords: Ugi-Zhu reaction; polyheterocycles; docking; COVID-19; SARS-CoV-2; main protease M^{Pro}

Citation: Morales-Salazar, I.; Castañón-Alonso, S.L.; Canseco-González, D.; Díaz-Cervantes, E.; González-Zamora, E.; Islas-Jácome, A. Synthesis of New *bis*-furanyl-pyrrolo[3,4-*b*]pyridin-5-ones via the Ugi-Zhu Reaction and Docking Studies on the Main Protease (M^{Pro}) from SARS-CoV-2. *Chem. Proc.* **2021**, *3*, x. https://doi.org/10.3390/xxxxx

Academic Editor: Julio A. Seijas

Published: date

1. Introduction

With the current pandemic COVID-19, it has become increasingly necessary to develop design-synthesis strategies based on robust computational methods behind understanding the response of the SARS-CoV-2 towards new candidate polyheterocyclic compounds for further in vitro antiviral activity studies. The rational drug design is a very valuable tool that minimizes the relationship between trial and error, providing some de novo design of antiviral compounds, including the use of nanocarriers [1–3]. Thanks to advances in areas such as organic physical chemistry, theoretical chemistry, computational chemistry, and pharmacochemistry, amazing algorithms can be implemented behind predict the interactions between an organic ligand and its biological receptor. A widely used methodology is the molecular docking, a simulation method that is complemented with results from in vitro assays to evaluate new compounds with potential biological activity. In February 2020, it was published the main protease from SARS-CoV-2

M^{pro} (PDB code: 6lu7) [4], which has an important role in both replication and transcription of virus [5].

Moreover, heterocyclic chemistry is a branch of organic chemistry of special interest. Heterocycles are found in a wide variety of products such as: drugs, natural products, agrochemicals, copolymers, materials, among others [6]. It is known that 90% of new drugs contain one or more heterocycles in their structure, so their importance in medicinal chemistry is crucial [7]. Isoindolin-1-one is a synthetic platform with biological properties incorporated into several products of pharmaceutical interest [8] (Figure 1a). An aza-analogue of this heterocyclic moiety is the pyrrolo[3,4-*b*]pyridin-5-one, found in many biological active compounds [9], analogues of natural products [10], and in some anticancer agents [11] (Figure 1b). Also, furan ring is contained in antibacterial, enzymatic inhibitors, antibiotics, antifungals, and so on [12,13] (Figure 1c).

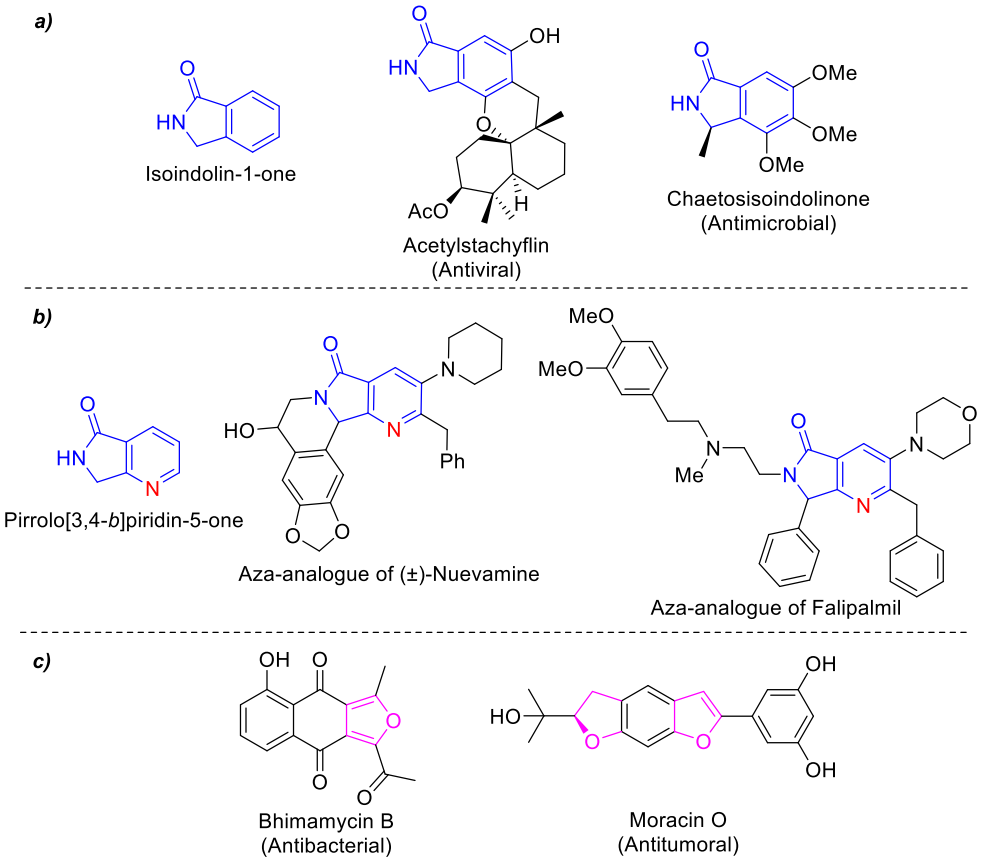

Figure 1. (**a**) Isoindolin-1-one and related natural products, (**b**) Pyrrolo[3,4-*b*]pyridin-5-ones and related bioactive compounds, and (**c**) Furan-based drugs.

Multicomponent reactions (MCRs) are powerful tools to synthesize quickly and efficiently novel polyheterocyclic compounds. MCRs belong to one-pot process and can be based on the use of isocyanides as principal reagents due to their duality as nucleophiles and electrophiles. MCRs are carried out directly or coupled to further transformations, for instance, ionic, pericyclic, radical-mediated, or metal-catalyzed [14]. Isocyanide-based multicomponent reactions let afford a wide variety of complexes polyheterocyclic whom applied in drug discovery [15]. A classic example that incorporates isocyanides in MCRs is three and four component-Ugi reaction [16]. Within the Ugi-type reactions, it has been recently published a variant of the Ugi reaction that has been studied in our research group called the Ugi-Zhu three-component reaction (UZ-3CR), useful mainly to synthesize 5-aminooxazoles that can act as synthetic platforms toward more complex polyheterocycles. The UZ-3CR involves the combination of aldehydes **1,** amines **2**, and aminoacid-

derived isocyanides **3** in protic or aprotic solvents to assemble just the oxazole core **4**. This MCR are eventually promoted by Lewis or Brønsted acids [17] (Scheme 1).

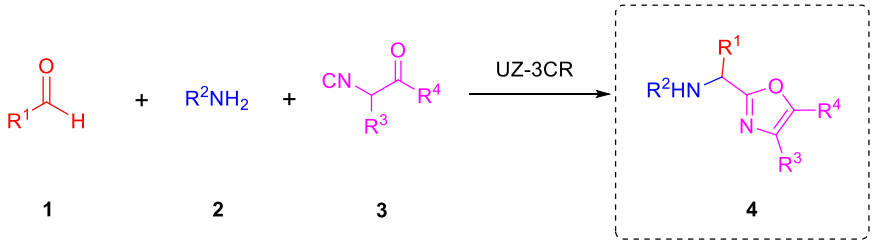

Scheme 1. The Ugi-Zhu three-component reaction.

2. Results and Discussion

2.1. Chemistry

To synthesize the desired *bis*-furanyl-pyrrolo[3,4-*b*]pyridin-5-ones **8a-e**, the UZ-3CR was coupled to a cascade process: *aza*-Diels-Alder/*N*-acylation/aromatization (decarboxylation/dehydration) into a one pot process. The first attempt was carried out under the Zhu's classic conditions [18], and then optimized several times in our research group [19,20]. It was found that initially dichloromethane as solvent and scandium triflate as Lewis acid catalyst worked well. However, the solvent used to synthesize all products was toluene due to better solubility observed for all reagents. It was necessary first to synthesize the isocyanides **3** from their corresponding aminoacids in three steps as reported also by Zhu and co-workers [18]. With the isocyanide in hands, according to the Ugi-Zhu mechanism, a condensation occurs between aldehydes **1a-b** and amines **2a-b** to access to imines **5a-e**, which become in Lewis' iminium ions **6a-e** after reacting with catalytic amount of scandium(III) triflate. The later intermediates are nucleophilically attacked by the isocyanides **3a-b** to give the 5-aminooxazoles **4a-e** via a non-prototropic chain-ring tautomerization. Subsequently, after adding maleic anhydride (**7**), an aza-Diels-Alder cycloaddition coupled into a cascade process *N*-acylation/aromatization (decarboxylation/dehydration) takes place to generate the corresponding pyrrolo[3,4-*b*]pyridin-5-ones **8a-e** in 24 to 40% yields (Scheme 2). It is worth highlighting the structural complexity of each product, as well as the formation of several new C-C and C-N bonds while leaving only one molecule of water and one of carbon dioxide, which denotes a high atomic economy and a green approach of this synthetic methodology. Also, the use of furan-substituted starting materials for the structural decoration of the pyrrolo [3,4-*b*] pyridin-5-one nucleus had not been reported yet in the literature.

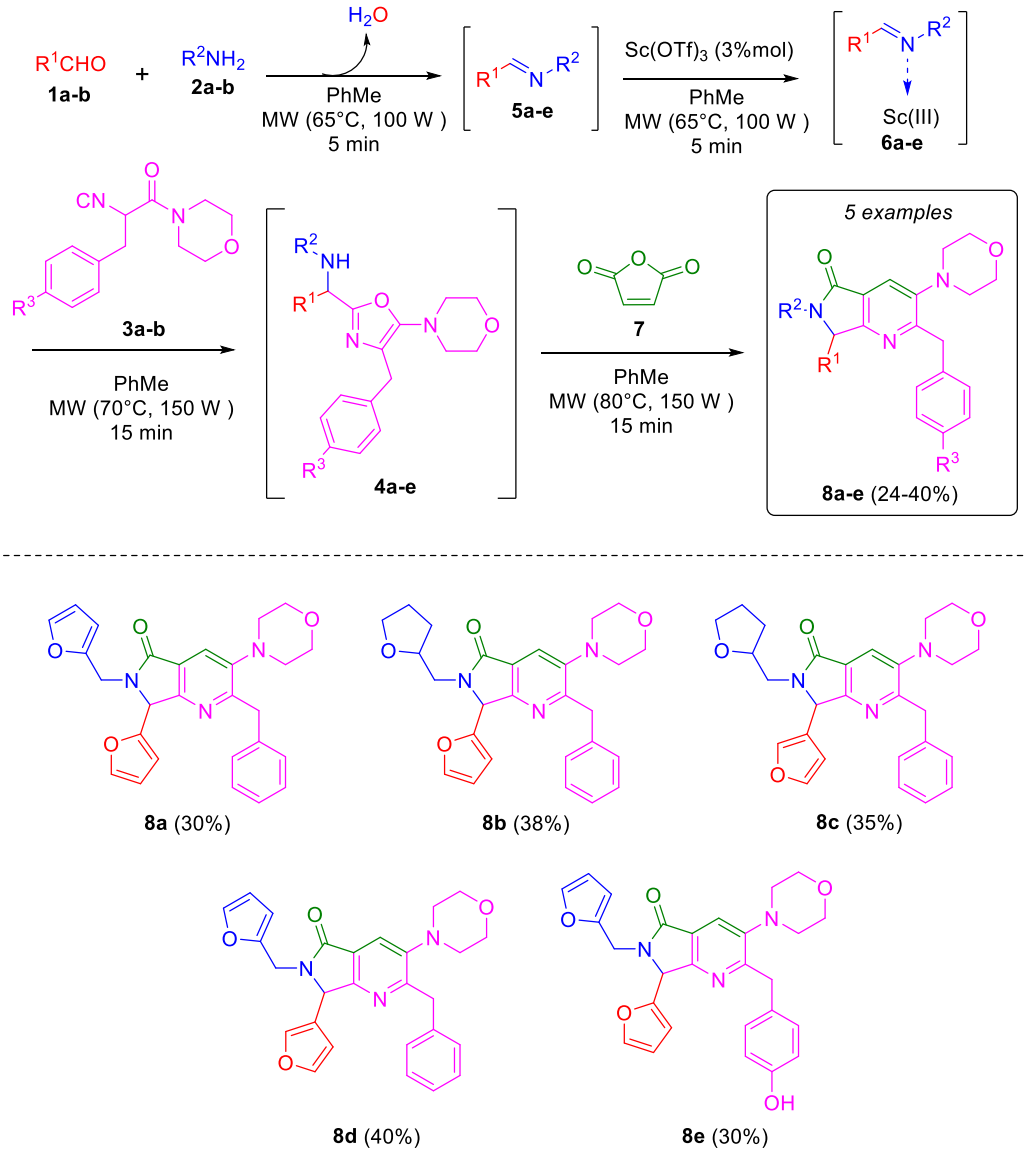

Scheme 2. Synthesis of pyrrolo[3,4-*b*]pyridin-5-ones via a cascade process (Ugi-Zhu/azaDiels-Alder/*N*-acylation/aromatization).

The products **8a-e** were characterized by ^{1}H and ^{13}C NMR (see the experimental part for further details). The 2-benzyl-7-(furan-2-yl)-6-(furan-2-ylmethyl)-3-morpholino-6,7-dihydro-5*H*-pyrrolo[3,4-*b*]pyridin-5-one (**8a**) was selected to show its spectrums on behalf of the series **8a-e**. With respect to the ^{1}H NMR spectrum, the key signals of pyrrolo[3,4-*b*]pyridin-5-one nucleus are two singlets, at 7.91 and 5.56 ppm, respectively, corresponding to position 4 of pyridine (*I*), and methyne (*II*). The diasterotopic methylene (*III*) emits also key signals, consisting of two doublets, at 5.22 and 4.06 ppm, respectively (Figure 2a). The difference in their chemical shifts is due to an influence from nitrogen lone pair, and to the stereogenic center (*II*). Thus, with respect to the ^{13}C NMR spectrum, the key peak is attributed to the carbonyl group (*IV*) at 166.3 ppm (Figure 2b).

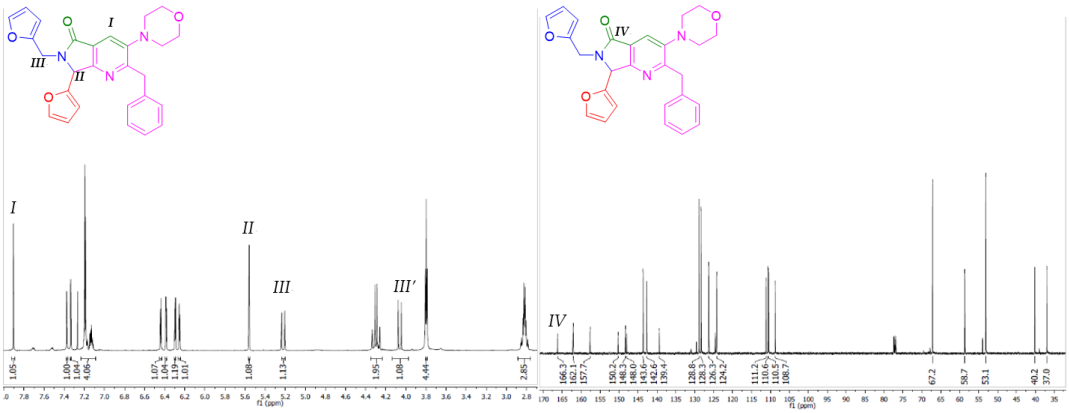

(**a**) (**b**)

Figure 2. (**a**) ^{1}H NMR spectrum of the compound **1a**, (**b**) ^{13}C NMR spectrum of the compound **8a**.

2.2. In Silico Study

Once molecular docking was performed on the active site of the SARS-CoV-2-M^{Pro}, which has been reported for our research group [1–3], the studied molecules were positioned as Figure 3 shows.

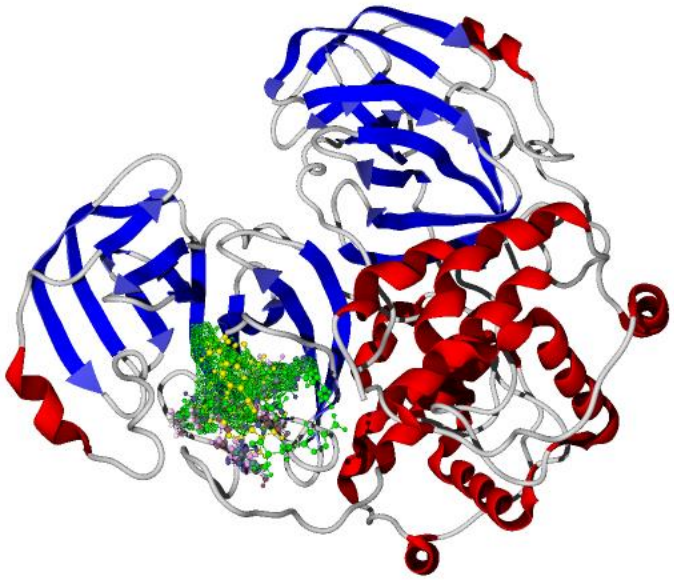

Figure 3. Molecular docking of the synthesized novel *bis*-furanyl-pyrrolo[3,4-*b*]pyridin-5-ones and two reference molecules.

The docking results show that all the synthesized molecules in the current work present exergonic interactions with the SARS-CoV-2-M^{Pro} (Table 1). Analyzing the results and considering that the more negative values indicate, the more stable ligand-target formed system, it is clear that **8c** is the molecule with a higher interaction with the SARS-CoV-2-M^{Pro}, with a ligand efficiency (LE) value of -5.96 kcal/mol. Note that P8 is a designed molecule by Díaz-Cervantes and co-workers, with a high ligand-target interaction against the SARS-CoV-2, and co-crystallized molecules are ligand experimental tested. Although the above molecules present high interactions, **8c** shows a better LE than the studied molecules depicted in Table 1.

8b and **8a** show a LE of −5.90 and −5.89 kcal/mol, respectively, which are almost degenerate with **8c**. This result denotes that the other synthesized molecules can also be considered potential drugs against the COVID-19.

Table 1. Main interaction energies between the studied molecules and the SARS-CoV-2-M^{Pro} *.

Ligand	E	LE	H bond	Electro	VdW
8a	−200.10	−5.89	−0.34	−0.07	−50.44
8b	−200.51	−5.90	−0.79	−1.25	−45.95
8c	−202.78	−5.96	−0.96	−0.54	−41.40
8d	−185.72	−5.46	−2.40	0.18	39.00
8e	−195.81	−5.59	−2.74	−0.85	0.56
co-crystal	−214.71	−4.38	−10.10	−0.08	−71.53
P8 [1]	−255.79	−5.44	−7.99	−0.11	−60.73

* All the values are represented in kcal/mol. E is the total ligand-target interaction; LE means the ligand efficiency (LE = E/#heavy atoms); H bond represent the hydrogen bond interactions; Electro is the electrostatic interactions and VdW thee Van de Waals interactions.

The Table 1 shows that smallest size of **8c** is a determinant factor to promotes a ligan-target interaction, due to H bond, electro and VdW energies are not the best for **8c** compared with the another studied ligands.

In this order, the hydrophilic interactions have been analyzed; see the Figure 4, which demonstrates that the hydrophobicity then promotes one essential interaction in this kind of target. The hydrophobic side of the target confers a higher site in the center of the cavity, which promotes better interactions by **8c**.

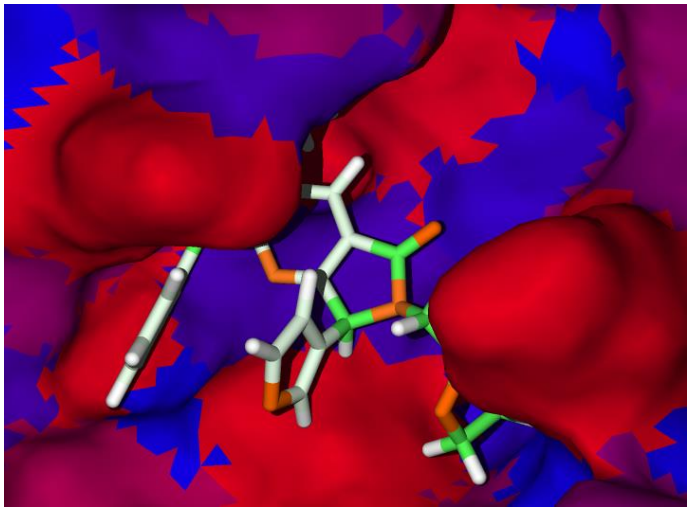

Figure 4. Hydrophobicity surfaces for **8c**. Red and blue surfaces represent the hydrophilic and hydrophobic surfaces of the SARS-CoV-2-M^{Pro}, respectively. Green and orange sticks are the hydrophilic and hydrophobic moieties of **8c**.

3. Conclusions

Considering the docking assay, the present studies demonstrate that **8c** can be considered as a drug candidate against the SARS-CoV-2-M^{Pro} due to its LE value (−5.96 kcal/mol), which is better than other synthesized and reported molecules. At the same time, the hydrophobic interaction plays a key role in the ligand targe molecular couplings, demonstrated through a hydrophobicity surfaces analysis. Finally, **8a** and **8b** can also be considered as drug candidates.

4. Experimental Section

4.1. General Information, Instrumentation and Chemicals

^{1}H and ^{13}C NMR spectra were acquired on a Bruker Advance III (500 MHz) spectrometer. The solvent was deuterated chloroform ($CDCl_3$). Chemical shifts are reported in parts per million (δ/ppm). Internal reference for NMR spectra is in respect to tetramethyl silane (TMS) at 0.0 ppm. Coupling constants are reported in Hertz (*J*/Hz). Multiplicities of the signals are reported using the standard abbreviations: singlet (s), doublet (d), triplet (t), quartet (q), and multiplet (m). NMR data were treated using the MestReNova software (12.0.0–20080). Microwave-assisted reactions were performed in closed-vessel mode on a CEM Discover MW-reactor (Matthews, North Carolina, CA, USA). Reaction progress was monitored by thin-layer chromatography (TLC) and the spots were visualized under ultraviolet (UV) light (254 or 365 nm). Flash columns packed with silica-gel 60 and glass preparative plates (20 × 20 cm) coated with silica-gel 60 doped with UV indicator (F254) were used to purify the products. Mixtures of hexanes (Hex) and ethyl acetate (EtOAc) in 1:1 or 1:2 (*v*/*v*) proportion were used to run TLC, silica-gel columns, preparative plates, and to measure the retention factor (Rf) values (using the same mobile phase for all the experiments). All starting reagents and solvents were used as received (without further purification, distillation, nor dehydration). Chemical structures were drawn using the ChemDraw Professional software (Ver. 15.0.0.106, Perkin Elmer Informatics, Cambridge, MA, USA). The purity for all synthesized products (>95%) was assessed by NMR.

4.2. Synthesis and Characterization of the bis-furanyl-pyrrolo[3,4-b]pyridine-5-ones **8a-e**

General Procedure (GP): The corresponding aldehydes **1a–b** (1.0 equiv.) and the amines **2a-b** (0.1 mmol, 1.0 equiv.) were placed in a sealed CEM Discover microwave reaction tube (10 mL) and diluted in toluene [1.0 mL]. Then, the mixture was stirred and heated using microwave irradiation (65 °C, 100 W) for 5 min, and scandium (III) triflate (0.03 equiv.) was added. The mixture was stirred and heated using microwave irradiation (65 °C, 100 W) for 5 min, and then the corresponding isocyanides **3a–b** (1.2 equiv.) were added. The new mixture was stirred and again heated using microwave irradiation (70 °C, 150 W) for 15 min, and then maleic anhydride (**7**) (1.4 equiv.) was added. Finally, the reaction mixture was stirred and heated using microwave irradiation (80 °C, 150 W) for 15 min. Then, the solvent was removed to dryness under vacuum. The crude was extracted using dichloromethane (3 × 25.0 mL) and $Na_2CO_{3\,(aq.)}$ (3 × 25 mL), and then washed with brine (3 × 25 mL). The organic layer was dried using anhydrous Na_2SO_4, filtered, and concentrated to dryness under vacuum. The new crude was purified by silica-gel column chromatography followed by preparative TLC using mixtures of hexanes (Hex) and ethyl acetate (EtOAc) in 1:1 or 1:2 (*v*/*v*) proportions as mobile phase to isolate the corresponding *bis*-furanyl-pyrrolo[3,4-*b*]pyridin-5-ones **8a-e** as racemic mixtures.

2-benzyl-7-(furan-2-yl)-6-(furan-2-ylmethyl)-3-morpholino-6,7-dihydro-5*H*-pyrrolo[3,4-*b*]pyridin-5-one (**8a**)

According to the GP, 2-furaldehyde (86 μL), 2-aminomethylfuran (92 μL), scandium (III) triflate (1.5mg), 2-isocyano-1-morpholino-3-phenylpropan-1-one (305mg), and maleic anhydride (143 mg) were reacted together in toluene (1.0 mL) to afford **8a** (30 mg, 30%) as a yellow oil; R_f = 0.38 (Hex–AcOEt = 1:1, *v*/*v*); ^{1}H NMR (500 MHz, $CDCl_3$): δ 7.91 (s, 1H), 7.37 (dd, *J* = 1.9, 0.9 Hz, 1H), 7.33 (dd, *J* = 1.9, 0.9 Hz, 1H), 7.24–7.09 (m, 4H), 6.44 (ddd, *J* = 3.3, 0.9, 0.3 Hz, 1H), 6.39 (dd, *J* = 3.3, 1.9 Hz, 1H), 6.30 (dd, *J* = 3.2, 1.9 Hz, 1H), 6.25 (dd, *J* = 3.2, 0.8 Hz, 1H), 5.56 (s, 1H), 5.22 (d, *J* = 15.7 Hz, 1H), 4.35–4.25 (m, 2H), 4.06 (d, *J* = 15.7 Hz, 1H), 3.80 (t, *J* = 4.6 Hz, 4H), 2.86–2.78 (m, 4H) ppm; ^{13}C NMR (125 MHz, $CDCl_3$): δ 166.3, 162.1, 157.7, 150.2, 148.3, 148.0, 143.6, 142.6, 139.4, 128.8, 128.3, 126.3, 124.2, 111.2, 110.6, 110.5, 108.7, 67.2, 58.7, 53.1, 40.2, 37.0 ppm.

2-benzyl-7-(furan-2-yl)-3-morpholino-6-((tetrahydrofuran-2-yl)methyl)-6,7-dihydro-5*H*-pyrrolo[3,4-*b*]pyridin-5-one (**8b**)

According to the GP, 2-furaldehyde (86 μL), 2-(aminomethyl)tetrahydrofuran (107 μL), scandium (III) triflate (1.5 mg), 2-isocyano-1-morpholino-3-phenylpropan-1-one (305 mg), and maleic anhydride (143 mg) were reacted together in toluene (1.0 mL) to afford **8b** (39 mg, 38%) as a yellow oil; R_f = 0.35 (Hex–AcOEt = 1:2, *v*/*v*); ^{1}H NMR (500 MHz, $CDCl_3$): δ 7.91 (s, 1H), 7.36 (ddd, *J* = 3.8, 1.9, 0.9 Hz, 1H), 7.22–7.11 (m, 5H), 6.47 (dd, *J* = 4.4, 3.3, Hz, 1H), 6.38 (dd, *J* = 3.3, 1.9 Hz, 1H), 5.82 (s, 1H), 4.37–4.27 (m, 2H), 4.06 (m, 2H), 3.91–3.83 (m, 1H), 3.80 (m, 4H), 2.82 (m, 4H), 1.87 (dd, *J* = 7.9, 6.8 Hz, 2H) ppm; ^{13}C NMR (125 MHz, $CDCl_3$): δ 167.1, 161.9, 158.0, 148.2, 143.5, 139.4, 128.9, 128.3, 126.3, 124.4, 111.4, 110.7, 67.3, 60.4, 53.2, 44.6, 43.2, 40.1, 29.4.

2-benzyl-7-(furan-3-yl)-3-morpholino-6-((tetrahydrofuran-2-yl)methyl)-6,7-dihydro-5*H*-pyrrolo[3,4-*b*]pyridin-5-one (**8c**)

According to the GP, 3-furancarboxaldehyde (90 μL), 2-(aminomethyl)tetrahydrofuran (107 μL), scandium (III) triflate (1.5 mg), 2-isocyano-1-morpholino-3-phenylpropan-1-one (305 mg), and maleic anhydride (143 mg) were reacted together in toluene (1.0 mL) to afford **8c** (37 mg, 35%) as a yellow oil; R_f = 0.20 (Hex–AcOEt = 1:1, *v*/*v*); ^{1}H NMR (500 MHz, $CDCl_3$): δ 7.89 (s, 1H), 7.62 (dd, *J* = 9.5, 1.6, Hz, 1H), 7.39–7.37 (m, 1H), 7.22–7.11 (m, 5H), 5.97 (dd, *J* = 1.9, 0.6 Hz, 1H), 5.72 (s, 1H), 4.38–4.25 (m, 2H), 4.12 (d, *J* = 7.2 Hz, 2H), 3.85 (m, 1H), 3.81 (dt, *J* = 4.3, 1.6 Hz, 4H), 2.82 (td, *J* = 5.9, 4.9, 2.6 Hz, 4H), 1.27–1.24 (m, 2H) ppm; ^{13}C NMR (125 MHz, $CDCl_3$): δ 167.2, 162.0, 160.0, 148.1, 143.9, 142.8, 139.4, 128.9, 128.3, 126.3, 124.5, 124.3, 120.2, 108.7, 68.0, 67.3, 58.2, 53.2, 44.3, 42.4, 40.2, 29.5. ppm.

2-benzyl-6-(furan-2-ylmethyl)-7-(furan-3-yl)-3-morpholino-6,7-dihydro-5*H*-pyrrolo[3,4-*b*]pyridin-5-one (**8d**)

According to the GP, 3-furancarboxaldehyde (90 μL), 2-aminomethylfuran (93 μL), scandium (III) triflate (1.5 mg), 2-isocyano-1-morpholino-3-phenylpropan-1-one (305 mg), and maleic anhydride (143 mg) were reacted together in toluene (1.0 mL) to afford **8d** (40.4 mg, 40%) as a yellow oil; R_f = 0.43 (Hex–AcOEt = 1:1, *v*/*v*); ^{1}H NMR (500 MHz, $CDCl_3$): δ 7.91 (s, 1H), 7.61 (ddd, *J* = 1.4, 0.9, 0.4 Hz, 1H), 7.41 (ddd, *J* = 2.0, 1.5, 0.5 Hz, 1H), 7.35 (dd, *J* = 1.9, 0.9 Hz, 1H), 7.22–7.11 (m, 5H), 6.31 (dd, *J* = 3.2, 1.9 Hz, 1H), 6.26 (d, *J* = 0.7 Hz, 1H), 6.03 (ddd, *J* = 1.9, 0.9, 0.4 Hz, 1H), 5.45 (s, 1H), 5.29 (s, 1H), 4.30 (d, *J* = 13.6 Hz, 2H), 4.03 (dt, *J* = 15.6, 0.5 Hz, 1H), 3.81 (t, *J* = 4.6 Hz, 4H), 2.82 (d, *J* = 5.3 Hz, 4H) ppm; ^{13}C NMR (125 MHz, $CDCl_3$) δ 166.2, 162.2, 159.5, 150.3, 148.1, 144.1, 142.6, 139.3, 128.8, 128.3, 126.3, 124.3, 120.0, 110.5, 108.7, 67.2, 56.9, 53.1, 40.1, 36.5 ppm.

7-(furan-2-yl)-6-(furan-2-ylmethyl)-2-(4-hydroxybenzyl)-3-morpholino-6,7-dihydro-5*H*-pyrrolo[3,4-*b*]pyridin-5-one (**8e**)

According to the GP, 2-furaldehyde (86 μL), 2-aminomethylfuran (93 μL), scandium (III) triflate (1.5 mg), 3-(3-hydroxyphenyl)-2-isocyano-1-morpholinopropan-1-one (325 mg), and maleic anhydride (143 mg) were reacted together in toluene (1.0 mL) to afford **1e** (30.3 mg, 30%) as a yellow oil; R_f = 0.29 (Hex–AcOEt = 1:2, *v*/*v*); ^{1}H NMR (500 MHz, $CDCl_3$): δ 7.90 (s, 1H), 7.38-7.37 (m, 1H), 7.34–7.33 (m, 1H), 7.21 (d, *J* = 8.8 Hz, 2H), 7.01 (d, *J* = 8.8 Hz, 2H), 6.44–6.43 (m, 1H), 6.39–6.38 (m, 1H), 6.31–6.29 (m, 1H), 6.26–6.24 (m, 1H), 5.55 (s, 1H), 5.22 (d, *J* = 16.1 Hz, 1H), 4.28 (d, *J* = 7.1 Hz, 2H), 4.06 (d, *J* = 15.7 Hz, 1H), 3.81 (s, 4H), 2.84 (d, *J* = 5.7 Hz, 4H) ppm; ^{13}C NMR (125 MHz, $CDCl_3$): δ 166.3, 161.8, 157.9, 153.8, 150.3, 149.7, 148.3, 148.0, 143.7, 142.7, 137.1, 129.9, 124.4, 120.9, 111.3, 110.7, 110.6, 108.8, 67.3, 58.7, 53.2, 39.5, 37.1 ppm.

4.3. Docking

The in-silico assay was carried out at molecular mechanics level, using the MolDock [21] scoring function through the Molegro virtual docker package [22] to perform the docking between the ligands and the SARS-CoV-2-M^{PRO}. Previously, the whole molecules were modeled and optimized using the Avogadro software [23].

Author Contributions: All authors contributed equally to this work. All authors have read and agreed to the published version of the manuscript.

Funding: A.I.-J. acknowledges "Proyecto Apoyado por el Fondo Sectorial de Investigación para la Educación CONACyT-SEP CB-2017-2018 (A1-S-32582)" and CBI-UAM-I Project (PAPDI2021_DQ 1) for financial support.

Institutional Review Board Statement: Not applicable.

Informed Consent Statement: Not applicable.

Acknowledgments: I.M.-S (947606) thanks CONACyT-México for her scholarship.

Conflicts of Interest: The authors declare no conflict of interest. The funders had no role in the design of the study; in the collection, analyses, or interpretation of data; in the writing of the manuscript, or in the decision to publish the results.

References

1. Cortés-García, C.J.; Chacón-García, L.; Mejía-Benavides, J.E.; Díaz-Cervantes, E. Tackling the SARS-CoV-2 main protease using hybrid derivatives of 1,5-disubstituted tetrazole-1,2,3-triazoles: An in silico assay. *PeerJ Phys. Chem.* **2020**, *2*, e10. https://doi.org/10.7717/peerj-pchem.10.
2. García-Ramírez, V.G.; Suarez-Castro, A.; Villa-Lopez, M.G.; Díaz-Cervantes, E.; Chacón-García, L.; Cortes-García, C.J. Synthesis of Novel Acylhydrazone-Oxazole Hybrids and Docking Studies of SARS-CoV-2 Main Protease *Chem. Proc.* **2021**, *3*, 1. https://doi.org/10.3390/ecsoc-24-08329.
3. Díaz-Cervantes, E.; Zenteno-Zúñiga, C.; Rodríguez-González, V.; Aguilera-Granja, F. Design of ZnO-Drug Nanocarriers against the Main Protease of SARS-CoV 2 (COVID-19): An In Silico Assay *Appl. Nano* **2021**, *2*, 257–266. https://doi.org/10.3390/applnano2030018.
4. Liu, X.; Zhang, B.; Jin, Z.; Yang, H.; Rao, Z. The crystal structure of COVID-19main protease in complex with an inhibitor N3. *Nature* **2020**, *582*, 289–293. https://doi.org/10.1038/s41586-020-2223-y.
5. Badavath, V.N.; Kumar, A.; Samanta, P.K.; Maji, S.; Das, A.; Blum, G.; Jha, A.; Sen, A. Determination of potential inhibitors based on isatin derivatives against SARS-CoV-2 main protease (Mpro): A molecular docking, molecular dynamics and structure-activity relationship studies. *J. Biomol. Struct. Dyn*. **2020**, 1–19. https://doi.org/10.1080/07391102.2020.1845800.
6. Arora, P.; Arora, V.; Lamba, H.S.; Wadhwa, D. Importance of heterocyclic chemistry: A review. *Int. J. Pharm. Res. Sci*. **2012**, *3*, 947–955.
7. Saini, M.S.; Kumar, A.; Dwivedi, J.; Singh, R. A review: Biological significances of heterocyclic compounds. *Int. J. Pharm. Sci. Res*. **2013**, *4*, 66–77.
8. Upadhyay, S.P.; Thapa, P.; Sharma, R.; Sharma, M. 1-Isoindolinone scaffold-based natural products with a promising diverse bioactivity. *Fitoterapia* **2020**, *146*, 104722. https://doi.org/10.1016/j.fitote.2020.104722.
9. Sun, X.; Janvier, P.; Zhao, G.; Bienaymé, H.; Zhu, J. A novel multicomponent synthesis of polysubstituted 5-aminooxazole and its new scaffold-generating reaction to pyrrolo[3,4-*b*]pyridine. *Org. Lett*. **2001**, *3*, 877–880, doi : 10.1021/ol007055q.
10. Vázquez-Vera, O.; Sánchez-Badillo, J.S.; Islas-Jácome, A.; Rentería-Gómez, M.A.; Pharande, S.G.; Cortes-García, C.J.; Rincón-Guevara, M.A.; Ibarra, I.A.; Gámez-Montaño, R.; González-Zamora, E. An efficient Ugi-3CR/aza Diels–Alder/Pomeranz–Fritsch protocol towards novel aza-analogues of (±)-nuevamine, (±)-lennoxamine and magallanesine: A diversity oriented synthesis approach. *Org. Biomol. Chem*. **2017**, *15*, 2363−2369. https://doi.org/10.1039/c6ob02572b.
11. Segura-Olvera, D.; García-González, A.N.; Morales-Salazar, I.; Islas-Jácome, A.; Rojas-Aguirre, Y.; Ibarra, I.A.; Díaz-Cervantes, E.; Alcaraz-Estrada, S.L.; González-Zamora, E. Synthesis of pyrrolo[3,4-*b*]pyridin-5-ones via multicomponent reactions and in vitro–in silico studies against SiHa, HeLa, and CaSki human cervical carcinoma cell lines. *Molecules* **2019**, *24*, 2648. https://doi.org/10.3390/molecules24142648.
12. Boto, A.; Alvarez, L. Furan and its derivatives. In *Heterocycles in Natural Product Synthesis*, 1st ed.; Majumdar, K.C., Chattopadhyay, S.K., Eds.; Wiley-VCH Verlag: Weinheim, Germany, 2011; pp. 99–107.
13. Chandrashekarachar, D.; Kesagudu, D. Importance of Furan Based Compounds and their Biomedical Applications: An Overview. *Indo Am. J. Pharm. Res.* **2017**, *7*, 7541–7549.
14. Ibarra, I.A.; Islas-Jácome, A.; González-Zamora, E. Synthesis of polyheterocycles via multicomponent reactions. *Org. Biomol. Chem.* **2018**, *16*, 1402–1418. https://doi.org/10.1039/c7ob02305g.
15. Váradi, A.; Palmer, T.C.; Dardashti, R.N.; Majumdar, S. Isocyanide-based multicomponent reactions for the synthesis of heterocycles. *Molecules* **2016**, *21*, 19–40. https://doi.org/10.3390/molecules21010019.
16. Lei, J.; Meng, J.-P.; Tang, D.-Y.; Frett, B.; Chen, Z.-Z.; Xu, Z.-G. Recent advances in the development of polycyclic skeletons via Ugi reaction cascades. *Mol. Divers*. **2018**, *22*, 503–516. https://doi.org/10.1007/s11030-017-9811-2.
17. Flores-Reyes, J.C.; Islas-Jácome, A.; González-Zamora, E. The Ugi three-component reaction and its variants. *Org. Chem. Front*. **2021**, *8*, 5460–5515. https://doi.org/10.1039/d1qo00313e.

18. Fayol, A.; Housseman, C.; Sun, X.; Janvier, P.; Bienaymé, H.; Zhu, J. Synthesis of α-Isocyano-α-alkyl(aryl)acetamides and their use in the multicomponent synthesis of 5-aminooxazole, pyrrolo[3,4-*b*]pyridin-5-one and 4,5,6,7-tetrahydrofuro[2,3-*c*]pyridine. *Synthesis* **2005**, *1*, 161−165. https://doi.org/10.1055/s-2004-831225.
19. Islas-Jácome, A.; Cárdenas-Galindo, L.E.; Jerezano, A.V.; Tamariz, J.; González-Zamora, E.; Gámez-Montaño, R. Synthesis of nuevamine aza-analogues by a sequence: I-MCR–Aza-Diels–Alder–Pictet–Spengler. *Synlett* **2012**, *23*, 2951–2956. https://doi.org/10.1055/s-0032-1317622.
20. Islas-Jácome, A.; Gutiérrez-Carrillo, A.; García-Garibay, M.A.; González-Zamora, E. One-pot synthesis of nuevamine aza-analogues by combined use of an oxidative Ugi type reaction and aza-Diels–Alder cycloaddition. *Synlett* **2014**, *25*, 0403–0406. https://doi.org/10.1055/s-0033-1340218.
21. Thomsen, R.; Christensen, M.H. MolDock: A new technique for high-accuracy molecular docking. *J. Med. Chem.* **2006**, *49*, 3315–3321.
22. Yang, J.; Chen, C. Gemdock: A generic evolutionary method for molecular docking. *Proteins* **2004**, *55*, 288–304.
23. Hanwell, M.; Curtis, D.; Lonie, D.; Vandermeersch, T.; Zurek, E.; Hutchison, G. Avogadro: An advanced semantic chemical editor, visualization, and analysis platform. *J. Cheminform.* **2012**, *4*, 17.